J. Biochem. 119, 857-862 (1996)

Kinetic Characterization of Antibody-Catalyzed Insertion of a Metal Ion into Porphyrin

Yasuko Kawamura-Konishi,* Naoki Hosomi,* Saburo Neya,† Sachiko Sugano,‡ Noriaki Funasaki,† and Haruo Suzuki*

**Department of Biosciences, School of Science and ‡Department of Biochemistry, School of Nursing, Kitasato University, Sagamihara, Kanagawa 228; and †Department of Physical Chemistry, Kyoto Pharmaceutical University, Yamashina, Kyoto 607*

Received for publication, November 13, 1995

The insertion of a copper(II) ion into mesoporphyrin by a monoclonal catalytic antibody has been investigated kinetically by measuring the increase in Soret absorbance due to the production of copper(II)-mesoporphyrin. The initial rate of the reaction showed saturation kinetics as a function of the mesoporphyrin concentration, while it increased linearly with an increase in the copper(II) concentration. Based on observations, a scheme for the reaction was proposed: mesoporphyrin binds to the antibody to form a complex, and copper(II) binds to the complex to yield copper(II)-mesoporphyrin. Kinetic parameters for the respective steps were estimated, and the thermodynamic parameters were calculated. The binding of mesoporphyrin to the antibody was endothermic and entropically driven. This implies that hydrophobic interactions are an important factor in the binding. Free energy profiles for the antibody-catalyzed and uncatalyzed reactions were drawn by use of the obtained thermodynamic parameter values. The results demonstrate that the rate acceleration by the antibody is ascribable to transition-state stabilization, and suggest that the structure of mesoporphyrin in the complex is more distorted than that of free mesoporphyrin.

Key words: abzyme, catalytic antibody, kinetics, porphyrin.

Since the first catalytic antibodies were generated in 1986 (*1, 2*), there have been nearly 80 reports about catalytic antibodies (*3, 4*). The mechanism by which these antibodies perform their catalytic functions has been postulated but largely remains unknown. Resolution of the mechanism will provide a way to augment their catalytic efficiency and to improve hapten design, and lead to understanding of the similarities and dissimilarities between natural enzymes and catalytic antibodies.

In this paper we report the kinetic characterization of an antibody-catalyzed reaction; the insertion of a copper(II) ion [Cu(II)] into mesoporphyrin (MP) to produce copper(II)-mesoporphyrin (Cu-MP). A monoclonal catalytic antibody (2B4) to *N*-methyl mesoporphyrin (*N*-MMP) was raised, according to the method reported by Cochran and Schultz (*5*), which mimicked the distorted porphyrin features of the transition state for the insertion of a metal ion into a planar porphyrin. We chose the antibody as a model for kinetic studies, since the product, metalloporphyrin, has a much larger absorption coefficient in the Soret region than the substrate, porphyrin (*6*), so the sensitivity of Soret absorption detection allows accurate kinetic measurements, particularly at low substrate concentrations. In addition, the antibody has the potential as a catalyst for other reactions, *e.g.*, redox or electron transfer reactions (*7, 8*), if it is bound tightly to iron-porphyrin derivatives. The kinetic and thermodynamic parameters obtained demonstrated the features of the antibody-catalyzed reaction.

Abbreviations: Cu(II), copper(II) ion; Cu-MP, copper(II) mesoporphyrin; DMSO, dimethyl sulfoxide; ELISA, enzyme-linked immunosorbent assay; KLH, keyhole limpet hemocyanin; MP, mesoporphyrin; *N*-MMP, *N*-methyl mesoporphyrin; OVA, ovalbumin.

MATERIALS AND METHODS

Synthesis—MP (*9*) and *N*-MMP (*10*) were prepared according to the reported methods. The *N*-MMP produced was a mixture of four structural isomers, with the methyl group for nitrogen atoms on pyrrole rings, in nearly equal amounts. Cu(II) was inserted into MP by refluxing a methanol solution containing two equivalents of Cu-$(CH_3CO_2)_2$ to afford Cu-MP with visible absorption peaks at 397, 524, and 561 nm. All of the porphyrin derivatives, purified by silica-gel chromatography, were identified on visible spectral comparison with the authentic ones. The concentrations of *N*-MMP, MP, and Cu-MP were determined by measuring the absorbance on the basis of absorption coefficients of 1.15×10^4 $M^{-1}\cdot cm^{-1}$ at 560 nm, 1.51×10^4 $M^{-1}\cdot cm^{-1}$ at 547 nm, and 2.57×10^4 $M^{-1}\cdot cm^{-1}$ at 561 nm, respectively (*6, 11*).

Preparation of KLH-Hapten and OVA-Hapten Conjugates—The hapten, *N*-MMP, was coupled to keyhole limpet hemocyanin (KLH) or ovalbumin (OVA) according to the following procedure. *N*-MMP (2.8 mg) was dissolved in 20 ml of distilled water. Water-soluble carbodiimide hydrochloride (310 mg; Peptide) and hydroxysulfosuccinimide (14.4 mg; Pierce) were then added to the solution.

The mixture was maintained for 30 min at pH 4.5-5.0 by the addition of 1 M HCl. After the reaction mixture had been neutralized with 1 M NaOH, KLH (2.5 mg; Calbiochem), or OVA (2.5 mg; Sigma) was added. The mixture was stirred for 6 h at 0°C, maintaining the pH at 8.0 by the addition of 1 M NaOH, dialyzed against PBS (8 mM Na_2HPO_4, 2 mM KH_2PO_4, 137 mM NaCl, and 3 mM KCl), and then lyophilized. The resultant KLH-hapten and OVA-hapten conjugates were dissolved in a small volume of PBS, respectively, and then stored at −20°C until used.

Antibody Production—BALB/c mice were immunized (hypodermic tail injection) with 50 μg of KLH-hapten emulsified in complete Freund's adjuvant. Fourteen days after the first injection, a booster (50 μg of KLH-hapten in incomplete Freund's adjuvant) was administered. Similar boosters were given two times at 14 days intervals. Six months after the first injection, a mouse was injected intravenously with 50 μg of KLH-hapten in PBS; 4 days later, the spleen cells were fused with a P3x 63AgU1 myeloma cell line according to the procedure of Masuho *et al.* (*12*). The hybridoma supernatants were screened by means of an ELISA technique for binding with OVA-hapten using a peroxidase-linked rabbit anti-mouse antibody (Zymed). Twenty-two supernatants were found to be positive on ELISA. Five of them contained antibodies of the IgM class, and the others ones of the IgG class. Fifteen IgG-secreting hybridoma cell lines were cloned. Two of the 15 monoclonal antibodies, 2B4 and 2D7, catalyzed the insertion of Cu(II) into MP to produce Cu(II)-MP at a rate above that of the background reaction.

Purification of a Catalytic Monoclonal Antibody—The 2B4 monoclonal antibody (IgG_{2a}, κ) was obtained by propagation of the respective clone as ascites in BALB/c mice. The globulin fraction was precipitated from the ascitic fluid by 20-50% ammonium sulfate fractionation. The ammonium sulfate was removed by dialysis against 20 mM phosphate buffer, pH 7.0. The antibody was next purified by affinity chromatography on a protein G-Sepharose (Pharmacia) column. After being loaded onto the column, unadsorbed materials were removed by extensive washing with 20 mM phosphate buffer, pH 7.0. The adsorbed antibody was eluted with 0.1 M citrate buffer, pH 3.0, immediately neutralized by the addition of a small volume of 2 M Tris-acetate, pH 9.0, and then dialyzed against 20 mM Tris-acetate buffer, pH 8.0. The antibody was next purified by anion exchange chromatography on a Resource Q (Pharmacia) column. The antibody was eluted with a linear gradient of NaCl, and then dialyzed against 0.1 M Tris-acetate buffer, pH 8.0. The purified antibody was judged to be homogeneous on SDS-PAGE under reducing conditions, exhibiting only heavy and light chains on Coomassie Blue staining. Protein concentrations were determined from the absorbance at 280 nm. The absorbance of 1% IgG was taken as 13.7 (*13*). The antibody concentration was expressed as active sites assuming a molecular weight of 150,000 (two active sites per antibody).

Measurement of Catalytic Activity—The initial rate for the monoclonal antibody catalyzed insertion of Cu(II) into MP was determined by measuring the increase in absorbance due to the production of Cu-MP. The 300 μl reaction mixtures contained 0.173-1.73 μM antibody, 5-90 μM MP, 0.15-1.5 mM copper(II) acetate (Nacalai Tesque), 0.5% (w/v) Triton X-100, and 5% DMSO in 90 mM Tris-acetate buffer, pH 8.0. Each reaction was initiated by the addition of Cu(II). The time course of the absorbance change was followed at 397 nm in a cuvette of 0.1 cm path length with a Hitachi U-3210 spectrophotometer equipped with HAAKE temperature controllers, F3 and CH. From the time course, the initial rate was calculated on the basis of the difference absorption coefficient at 397 nm between MP and Cu-MP, 0.318 $\mu M^{-1} \cdot cm^{-1}$, and expressed as μM Cu-MP produced per minute. The initial rates obtained were corrected for the background rate, which was determined under conditions identical to those for the antibody-catalyzed reaction.

Reverse-Phase HPLC—The 200 μl reaction mixture contained 0.864 μM antibody, 45 μM MP, 1 mM Cu(II), 0.5% (w/v) Triton X-100, and 5% DMSO in 90 mM Tris-acetate buffer, pH 8.0. The mixture was incubated at 37°C, and 20 μl aliquots of the mixture were poured into 80 μl 30% (v/v) DMSO in methanol containing 215 μM EDTA. After filtration, 50 μl of the solution was analyzed by HPLC. The chromatographic system consisted of a JASCO 880-PU pump, and a JASCO 880-30 solvent module equipped with a JASCO 875-UV/VS detector and an Inertsil C18 column (4.6 mm × 25 cm, 10 μm particle size; GL Science). The flow rate was 0.5 ml/min, and the absorbance at 400 nm was monitored. The amount of Cu-MP produced was determined using a standard curve generated with known amounts of Cu-MP.

Determination of the Dissociation Constant—The dissociation constant (K_d) of the *N*-MMP·antibody equilibrium was determined by the method of Friguet *et al.* (*14*) as follows. *N*-MMP at various concentrations ($[N\text{-MMP}]_t$ = 2.35 to 9.95 nM) was incubated with a constant concentration of the antibody ($[Ab]_t$ = 7.25 nM) in 90 mM Tris-acetate buffer, pH 8.0, containing 0.5% (w/v) Triton X-100 and 5% DMSO. After one hour incubation at 37°C, the amounts of free antibody were determined by measuring the absorbance by the ELISA technique described in the *Antibody Production* section. The K_d value was obtained by use of the following equation:

$$A_0/(A_0-A)-1=K_d/\{[N\text{-MMP}]_t-[Ab]_t\cdot(A_0-A)/A_0\}$$

where A and A_0 are the absorbance measured in the presence and absence of *N*-MMP, respectively, at 405 nm.

RESULTS

Kinetic Measurements—For kinetic characterization of a reaction, it is necessary to measure the initial rate of the reaction accurately. Since metalloporphyrin has a much larger absorption coefficient in the Soret region than porphyrin (*6*), the insertion of Cu(II) into MP to produce Cu-MP was detected by measuring the increase in the Soret absorption. Figure 1 shows the absorption changes at 397 nm after mixing of MP and Cu(II) in the presence and absence of monoclonal antibody 2B4, and the amounts of Cu-MP produced were calculated by use of the difference absorption coefficient of 0.318 $\mu M^{-1} \cdot cm^{-1}$ between Cu-MP and MP. To make sure that such a calculation was valid, the reaction mixture in the presence of the antibody was also analyzed by reverse-phase HPLC, and the results are presented in the same figure. The HPLC data agreed well with the time course. This showed that the insertion of

Cu(II) into MP to produce Cu-MP could be quantitated by measuring the increase in the Soret absorption, and the initial rate of the reaction could be exactly calculated from the time course.

Figure 2 shows the initial rate of the insertion of Cu(II) into MP as a function of the antibody concentration. A linear relationship was observed, indicating that the reaction was mediated by the antibody. The initial rate at 1 mM Cu(II) showed saturation kinetics as a function of the MP concentration (Fig. 3). Such kinetics were also observed at various Cu(II) concentrations (data not shown). These observations indicate that the reaction proceeds with Michaelis-Menten type kinetics. On the other hand, the initial rate increased linearly with an increase in the Cu(II) concentration (Fig. 4), and did not show a saturation curve at the Cu(II) concentrations studied, indicating that the reaction proceeds with second-order kinetics.

Based on the above observations, the following scheme may be proposed, which is essentially consistent with that of Cochran and Schultz (*5*), except that theirs includes

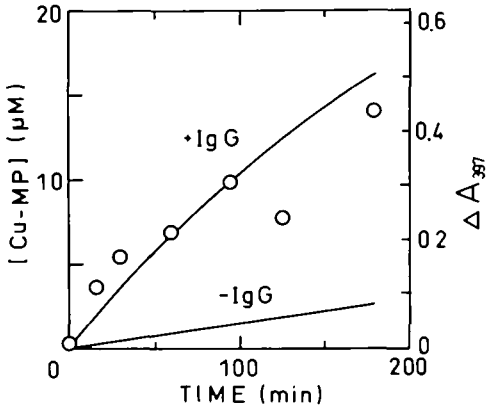

Fig. 1. **Time courses of antibody-catalyzed and uncatalyzed insertion of Cu(II) into MP to produce Cu-MP.** The reaction mixture contained 1 mM copper(II) acetate, 45 μM MP, 0.5% (w/v) Triton X-100, 5% (v/v) DMSO, and 90 mM Tris acetate (pH 8.0), at 37°C. The antibody concentration was 0.864 μM. Solid lines denote the absorbance change at 397 nm, and open circles show the HPLC analysis data (see text, and "MATERIALS AND METHODS").

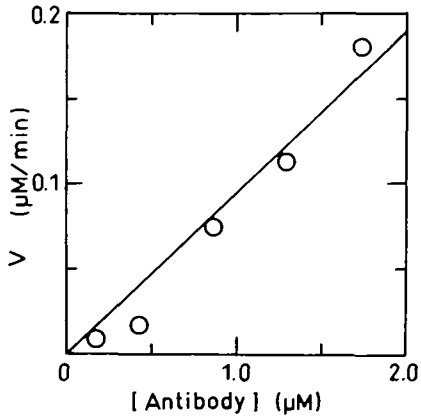

Fig. 2. **Relationship between the initial rate and the antibody concentration.** The concentration of antibody is expressed per binding site. The reaction mixture contained 1 mM copper(II) acetate, 36 μM MP, 0.5% (w/v) Triton X-100, 5% (v/v) DMSO, and 90 mM Tris acetate (pH 8.0), at 37°C.

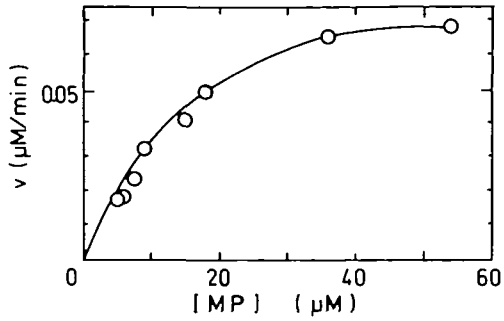

Fig. 3. **Relationship between the initial rate and the MP concentration.** The reaction mixture contained 0.864 μM antibody, 1 mM copper(II) acetate, 0.5% (w/v) Triton X-100, 5% (v/v) DMSO, and 90 mM Tris acetate (pH 8.0), at 37°C.

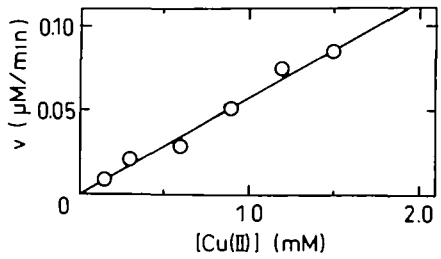

Fig. 4. **Relationship between the initial rate and the copper(II) acetate concentration.** The reaction mixture contained 0.864 μM antibody, 24 μM MP, 0.5% (w/v) Triton X-100, 5% (v/v) DMSO, and 90 mM Tris acetate (pH 8.0), at 37°C.

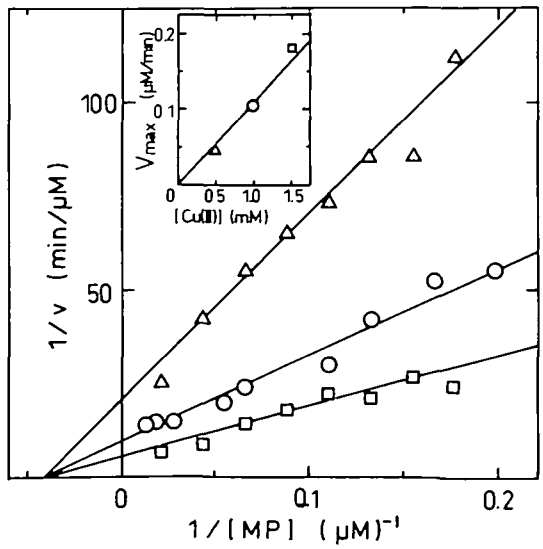

Fig. 5. **Double reciprocal plots of the initial rate *vs.* MP concentration at three different concentrations of copper(II) acetate (□: 1.5 mM, ○: 1.0 mM, △: 0.5 mM).** The reaction mixture contained 0.864 μM antibody, 0.5% (w/v) Triton X-100, 5% (v/v) DMSO, and 90 mM Tris acetate (pH 8.0), at 37°C. (Inset) Relationship between the reciprocal of the intercept on the ordinate of Fig. 5, V_{max}, *vs.* concentration of copper(II) acetate. From the slope of the plot, the *k* value was estimated to be 127 $M^{-1} \cdot s^{-1}$ using the antibody concentration of 0.864 μM.

TABLE I. **Kinetic parameters for insertion of Cu(II) into MP.**

Temperature (°C)	K_s (μM)	k ($M^{-1}\cdot min^{-1}$)	K_i (μM)
	Antibody-catalyzed reaction		
25	32.8±12.6	59.4±10.2	5.0±0.88
30	28.6±15.0	84.5±20.0	5.9±0.99
37	23.0±11.1	127±25.5	9.9±2.6
26[a]	50	72.2	—
	Uncatalyzed reaction		
25	—	0.15±0.032	—
30	—	0.21±0.036	—
37	—	0.28±0.040	—

[a]Data from Ref. 5. Each error is the standard deviation.

product inhibition, as described later. In the scheme, MP binds to the antibody (Ab) reversibly to form the complex (Ab·MP), followed by the binding of Cu(II) to the complex according to the second-order rate law. The binding of Cu(II) in turn dissociates the complex into the antibody and Cu-MP.

$$Ab + MP \underset{K_s}{\rightleftharpoons} Ab\cdot MP \quad (1)$$

$$K_s = [Ab]\,[MP]/[Ab\cdot MP] \quad (2)$$

$$Ab\cdot MP + Cu(II) \xrightarrow[k]{} Ab + Cu\text{-}MP \quad (3)$$

where K_s the dissociation constant of the complex and k the second-order rate constant for the Cu(II) binding. The rate of the increase in [Cu-MP], v, is derived from Eq. 3, as

$$v = d[Cu\text{-}MP]/dt = k[Cu(II)]\,[Ab\cdot MP] \quad (4)$$

When [Ab·MP] and [Cu-MP] are negligibly small as compared with [MP], Eq. 4 becomes Eq. 5 using the initial value of [Ab], $[Ab]_0$, and that of [MP], $[MP]_0$.

$$v = k[Cu(II)]\,[Ab]_0[MP]_0/(K_s + [MP]_0) \quad (5)$$

Equation 5 means that a plot of $1/v$ *vs.* $1/[MP]_0$ gives a straight line with the intercept on the abscissa as $-1/K_s$, and that on the ordinate as $1/(k[Cu(II)]\,[Ab]_0)$.

Figure 5 shows double reciprocal plots of v against $[MP]_0$ at various Cu(II) concentrations. It was found that there is a linear relationship between them, and each line gives the same intercept on the abscissa of the plots. The parameter, K_s, was determined to be 23 μM from the intercept value. The Fig. 5 inset shows the linear relationship between the reciprocal of the intercept on the ordinate of Fig. 5, V_{max}, *vs.* [Cu(II)]. From the slope of the plot, the k value was estimated to be 127 $M^{-1}\cdot min^{-1}$ using the antibody concentration of 0.864 μM. The obtained values of K_s and k, which are listed in Table I, were similar to those reported by Cochran and Schultz (*5*).

The natural enzyme, ferrochelatase (protoheme ferrolyase, EC 4.99.1.1), catalyzes the insertion of ferrous iron, Fe(II), into protoporphyrin to produce protoheme. The enzyme also catalyzes the insertion of various divalent metal ions into mesoporphyrin, but not that of Cu(II) (*15*). The K_m value of the enzyme was reported to be 26.7 μM for mesoporphyrin with Fe(II) (*16*). Interestingly, the K_s value of the antibody, 23 μM, is similar to the K_m value of the enzyme in spite of the difference in the metal ion. The catalytic activity of the antibody strongly depends on the second-order process for the binding of Cu(II) (Eq. 3), *i.e.* the rate of the binding is very slow with low concentrations of Cu(II). Acceleration of the binding of Cu(II) is necessary for improvement of the catalytic activity.

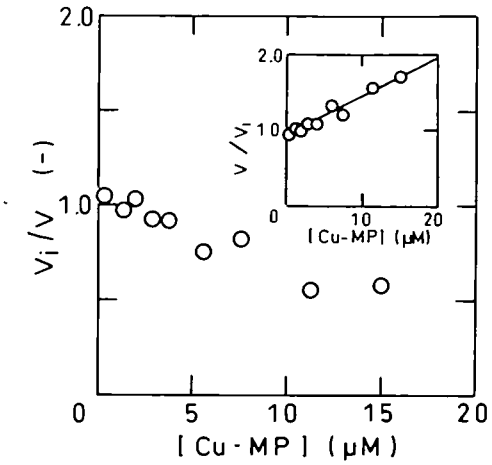

Fig. 6. **Inhibition of the insertion of Cu(II) into MP by Cu-MP.** The reaction mixture contained 0.864 μM antibody, 1 mM copper(II) acetate, 24 μM MP, 0.5% (w/v) Triton X-100, 5% (v/v) DMSO, 90 mM Tris acetate (pH 8.0) and 0.28–15 μM Cu-MP, at 37°C. A plot of v_i/v (or v/v_i, inset) and Cu-MP concentration is presented.

Product Inhibition—Cochran and Schultz (*5*) observed that catalytic activity was inhibited by the addition of various metalloporphyrins. To examine the possibility of product inhibition by Cu-MP, the initial rate was measured in the presence of 0.28–15 μM Cu-MP (Fig. 6). This figure shows that Cu-MP inhibited the reaction. The type of inhibition could not be determined, since further measurements could not be carried out at higher Cu-MP concentrations due to the high absorbance of the reaction mixture. On the assumption that Cu-MP competed with MP for binding to the antibody, the data in Fig. 6 were analyzed with the following equations.

$$Ab + Cu\text{-}MP \underset{K_i}{\rightleftharpoons} Ab\cdot Cu\text{-}MP \quad (6)$$

$$K_i = [Ab]\,[Cu\text{-}MP]/[Ab\cdot Cu\text{-}MP] \quad (7)$$

$$v/v_i = ([Cu\text{-}MP]/K_i)/(1 + [MP]_0/K_s) + 1 \quad (8)$$

where Ab·Cu-MP is the complex of the antibody and Cu-MP, K_i the dissociation constant of the complex, and v and v_i the initial rates in the absence and presence of Cu-MP, respectively. The Fig. 6 inset shows plots of v/v_i *vs.* [Cu-MP] using the data in Fig. 6. The slope of the plots gives $1/\{K_i\,(1 + [MP]_0/K_s)\}$. The K_i value was estimated to be 9.9 μM by use of a K_s value of 23 μM (Table I). Though Cu-MP is an inhibitor at concentrations comparable to those of MP, it does not significantly alter the rate when the concentration of Cu-MP is much lower than that of MP. For example, the concentration of Cu-MP produced was 1.8 μM at 10 min in the time course in Fig. 1, and the inhibition of Cu-MP was determined to be $v_i/v = 0.94$. Therefore, it seems likely that the observed initial rate was unaffected by product inhibition.

DISCUSSION

To reveal the features of the antibody-catalyzed insertion of Cu(II) into MP to produce Cu-MP, thermodynamic parameters of the reaction were calculated using the kinetic

TABLE II. **Thermodynamic parameters for insertion of Cu(II) into MP at 37°C.**

Reaction	Antibody-catalyzed			Uncatalyzed		
Parameter	ΔG_s	ΔH_s	ΔS_s			
$1/K_s$	-6.6 ± 0.32	5.2 ± 0.35	38 ± 2.2		—	
	$\Delta G^{\ddagger}_{cat}$	$\Delta H^{\ddagger}_{cat}$	$\Delta S^{\ddagger}_{cat}$	$\Delta G^{\ddagger}_{uncat}$	$\Delta H^{\ddagger}_{uncat}$	$\Delta S^{\ddagger}_{uncat}$
k^a	22 ± 0.20	11 ± 0.54	-35 ± 2.4	25.7 ± 0.10	9.9 ± 1.5	-51 ± 5.2
	ΔG_I	ΔH_I	ΔS_I			
K_I	7.1 ± 0.17	11 ± 3.1	11 ± 10		—	

ΔG, ΔH, and ΔS are the free energy change (kcal/mol), the enthalpy change (kcal/mol), and the entropy change (cal/mol/deg), respectively. The superscript, ‡, denotes activation. Each error is the standard deviation. [a] The k value was used as the first-order rate constant at [Cu(II)] = 1 mM.

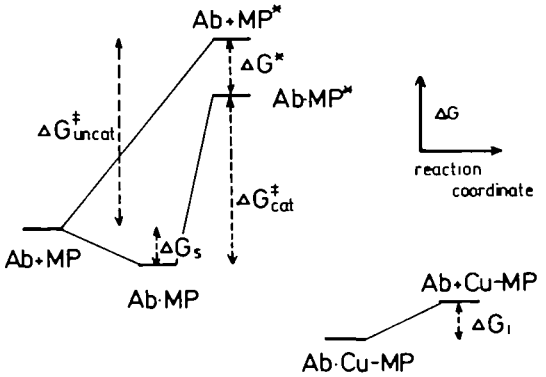

Fig. 7. **Free energy profile for the insertion of Cu(II) into MP to produce Cu-MP based on the results in Table II.** The standard concentration of Cu(II) is 1 mM and the temperature is 37°C. The subscript, *, denotes the transition-state.

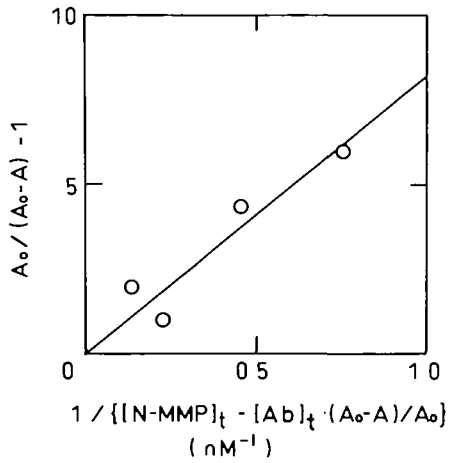

Fig. 8. **Plot of $A_0/(A_0-A)-1$ *vs.* $K_d/\{[N\text{-MMP}]_t-[\text{Ab}]_t\cdot(A_0-A)/A_0\}$.** A and A_0 are the absorbance at 405 nm, measured by the ELISA technique, in the absence and presence of N-MMP, respectively. $[N\text{-MMP}]_t$ and $[\text{Ab}]_t$ are the total concentrations of N-MMP and the antibody, respectively.

parameters in Table I. ΔG, ΔH, and ΔS for the binding of MP and Cu-MP to the antibody were calculated from van't Hoff plots of $1/K_s$ and $1/K_I$, respectively, and $\Delta G^{\ddagger}$, $\Delta H^{\ddagger}$, and $\Delta S^{\ddagger}$ for the binding of Cu(II) from Arrhenius plots of k at [Cu(II)] = 1 mM. The results are presented in Table II and discussed below. In the absence of the antibody, the reaction proceeded with second-order kinetics (data not shown), and the second-order rate constant and the thermodynamic parameters were calculated by the same procedure, and are listed in Tables I and II, respectively.

For the binding of MP to the antibody, $\Delta H_s = 5.2$ kcal/mol and $\Delta S_s = 38$ cal/mol/deg, as calculated using $1/K_s$, are shown in Table II. When two molecules bind to form one molecule, a negative ΔS is expected. The positive ΔS_s obtained suggests that water molecules are released when MP binds to the antibody. This implies that hydrophobic interactions are an important factor in the binding. The result of the negative ΔG_s was that the magnitude of the $T\cdot\Delta S_s$ factor exceeded that of ΔH_s. Therefore, the binding of MP to the antibody was entropically driven. In contrast to our results, negative ΔH and ΔS have been observed for the binding of some antibodies with the respective antigens (*17-19*). These bindings are enthalpically driven, and might include van der Waals interactions and hydrogen bonds.

Table II shows that the $\Delta H^{\ddagger}$ and $\Delta S^{\ddagger}$ values of the binding of Cu(II) to MP in the antibody-catalyzed reaction are 11 kcal/mol and -35 cal/mol/deg, respectively, and those in the uncatalyzed reaction are 9.9 kcal/mol and -51 cal/mol/deg, respectively. The rate acceleration by the antibody in this binding is ascribable to the entropy effect. The difference in $\Delta G^{\ddagger}$ between the antibody-catalyzed and uncatalyzed reactions is 4 kcal/mol. This value can be calculated to be a difference in equilibrium constant of about 660 times at 37°C, indicating that MP in the antibody-MP complex is activated more easily than free MP.

Negative ΔH, and ΔS are expected on dissociation of the antibody·Cu-MP complex into the antibody and Cu-MP, since this process includes the release of apolar Cu-MP into a polar solvent. However, as shown in Table II, both ΔH_I and ΔS_I are positive. The results suggest that interactions between the antibody and Cu-MP are not similar to those between the antibody and MP, which might be hydrophobic. The $T\cdot\Delta S_I$ factor is not large enough to compensate for the positive ΔH_I, resulting in a positive ΔG_I.

From the thermodynamic parameters in Table II, a free energy profile for the insertion of Cu(II) into MP to produce Cu-MP was drawn (Fig. 7). It was found that the favorable binding of MP to the antibody contributes to the rate acceleration by the antibody rather than the increased rate of the Cu(II) binding step. The difference in free energy between the transition state of free MP and that of the MP bound to the antibody, $\Delta G^*(=\Delta G^{\ddagger}_{uncat}-\Delta G_s-\Delta G^{\ddagger}_{cat})$, was calculated to be 10.3 ± 0.62 kcal/mol. To compare this value with the free energy change of the binding of N-MMP to the antibody, $\Delta G_{N\text{-MMP}}$, the dissociation constant of N-MMP, K_d, was determined by the ELISA method (Fig. 8). The K_d value obtained (8.20 ± 2.0 nM) gave the value of

$\Delta G_{N\text{-MMP}}$, -11.5 ± 0.15 kcal/mol, which was close to that of $-\Delta G^{*}$ (-10.3 ± 0.62 kcal/mol). This result indicates the validity of the free energy profile presented in Fig. 7, and that the antibody-catalyzed reaction is based upon the transition-state stabilization theory (*20, 21*). In addition, the value of $-\Delta G^{*}$ is smaller than that of ΔG_{s} by about 4 kcal/mol. These findings suggest that the structure of MP in the complex is similar to that in the transition-state, that is, MP in the complex is more distorted than free MP.

This work demonstrated that the rate acceleration by the antibody is ascribable to transition-state stabilization. Human ferrochelatase has a distinct histidine residue which might act as the binding site with a metal ion (*22*). The introduction of such residues as histidine in ferrochelatase into the active site in the antibody would be effective for improvement of the catalytic efficiency of the antibody. One question still remains, what is the difference between the catalytic antibody and the uncatalytic antibody raised to the same hapten, *N*-MMP. There should be differences in the affinity for the substrate, MP, the orientation of MP in the antibody-MP complex, the degree of porphyrin distortion, and/or the affinity for the product, Cu-MP, *etc.* To reveal the differences, further experiments are now in progress.

We wish to express our gratitude to Dr. Shu-ichi Tamauchi, Department of Microbiology, Kitasato University School of Medicine, for his valuable suggestion, and to Ms. E.B. Mukouyama in our laboratory for her help in the production of the monoclonal antibody. We also thank Miss A. Asano for her assistance in the ELISA.

REFERENCES

1. Tramontano, A., Janda, K.D., and Lerner, R.A. (1986) Catalytic antibodies. *Science* **234**, 1556-1570
2. Pollack, S.J., Jacobs, J.W., and Schultz, P.G. (1986) Selective chemical catalysis by an antibody. *Science* **234**, 1570-1573
3. Suzuki, H. (1994) Recent advances in abzyme studies. *J. Biochem.* **115**, 623-628
4. Guo, J., Huang, W., and Scanlan, T.S. (1994) Kinetic and mechanistic characterization of an efficient hydrolytic antibody: Evidence for the formation of an acyl intermediate. *J. Am. Chem. Soc.* **116**, 6062-6069
5. Cochran, A.G. and Schultz, P.G. (1990) Antibody-catalyzed porphyrin metallation. *Science* **249**, 781-783
6. Falk, J.E. (1964) Absorption spectra in *B.B.A. Library 2, Porphyrins and Metalloporphyrins*, pp. 231-246, Elsevier Publishing, Amsterdam
7. Cochran, A.G. and Schultz, P.G. (1990) Peroxidase activity of an antibody-heme complex. *J. Am. Chem. Soc.* **112**, 9414-9415
8. Keinan, E., Sinha, S.C., Shinha-Bagchi, A., Benory, E., Ghozi, M.C., Eshhar, Z., and Green, B.S. (1990) Towards antibody-mediated metallo-porphyrin chemistry. *Pure Appl. Chem.* **62**, 2013-2019
9. Baker, E.W., Ruccia, M., and Corwin, A.H. (1964) The preparation of mesoporphyrin IX and etioporphyrin III. *Anal. Biochem.* **8**, 512-518
10. Cavaleiro, J.A.S., Condesso, M.F.P.N., Jackson, A.H., Neves, M.G.P.M.S., Nagaraja Rao, K.R., and Sadashiva, B.K. (1984) Synthesis of *N*-monoalkylporphyrins. *Tetrahedron Lett.* **25**, 6047-6048
11. Lavallee, D.K. (1987) Visible-UV absorption spectroscopy in *The Chemistry and Biochemistry of N-Substituted Porphyrins*, pp. 41-53, VCH Publishers, New York
12. Masuho, Y., Sugano, T., Matsumoto, Y., Sawada, S., and Tomibe, K. (1986) Generation of hybridomas producing human monoclonal antibodies against herpes simplex virus after *in vitro* stimulation. *Biochem. Biophys. Res. Commun.* **135**, 495-500
13. Campbell, D.A., Gong, B., Kochersperger, L.M., Yonkovich, S., Gallop, M.A., and Schultz, P.G. (1994) Antibody-catalyzed prodrug activation. *J. Am. Chem. Soc.* **116**, 2165-2166
14. Friguet, B., Chaffotte, A.F., Djavadi-Ohaniance, L., and Goldberg, M.E. (1985) Measurements of the true affinity constant in solution of antigen-antibody complexes by enzyme-linked immunosorbent assay. *J. Immunol. Methods* **77**, 305-319
15. Taketani, S. (1994) Molecular and genetic characterization of ferrochelatase in *Regulation of Heme Protein Synthesis*, pp. 41-54, AlphaMed Press, OH
16. Taketani, S. and Tokunaga, R. (1981) Rat liver ferrochelatase. *J. Biol. Chem.* **256**, 12748-12753
17. Raman, C.S., Allen, M.J., and Nall, B.T. (1995) Enthalpy of antibody-cytochrome *c* binding. *Biochemistry* **34**, 5831-5838
18. Schwarz, F.P., Tello, D., Goldbaum, F.A., Mariuzza, R.A., and Poljak, R.J. (1995) Thermodynamics of antigen-antibody binding using specific anti-lysozyme antibodies. *Eur. J. Biochem.* **228**, 388-394
19. Shimba, N., Torigoe, H., Takahashi, H., Masuda, K., Shimada, I., Arata, Y., and Sarai, A. (1995) Comparative thermodynamic analyses of the Fv, Fab* and Fab fragments of anti-dansyl mouse monoclonal antibody. *FEBS Lett.* **360**, 247-250
20. Stewart, J.D. and Benkovic, S.J. (1995) Transition-state stabilization as a measure of the efficiency of antibody catalysis. *Nature* **375**, 388-391
21. Jahangiri, G.K. and Reymond, J.-L. (1994) Antibody-catalyzed hydrolysis of enol ethers. 2. Structure of the antibody-transition state complex and origin of the enantioselectivity. *J. Am. Chem. Soc.* **116**, 11264-11274
22. Kohno, H., Okuda, M., Furukawa, T., Tokunaga, R., and Taketani, S. (1994) Site-directed mutagenesis of human ferrochelatase: Identification of histidine-263 as a binding site for metal ions. *Biochim. Biophys. Acta* **1209**, 95-100